Mon. Not. R. Astron. Soc. **000**, 1–?? (2012) Printed 18 August 2016 (MN LATEX style file v2.2)

The Large Magellanic Cloud as a laboratory for Hot Bottom Burning in massive Asymptotic Giant Branch stars

P. Ventura[1], A. I. Karakas[2], F. Dell'Agli[1,3], M. L. Boyer[4,5], D. A. García–Hernández[6,7], M. Di Criscienzo[1], R. Schneider[1]

[1] *INAF – Osservatorio Astronomico di Roma, Via Frascati 33, 00040, Monte Porzio Catone (RM), Italy*
[2] *Research School of Astronomy and Astrophysics, Australian National University, Canberra, ACT 2611, Australia*
[3] *Dipartimento di Fisica, Università di Roma "La Sapienza", P.le Aldo Moro 5, 00143, Roma, Italy*
[4] *Observational Cosmology Lab, Code 665, NASA Goddard Space Flight Center, Greenbelt, MD 20771, USA*
[5] *Oak Ridge Associated Universities (ORAU), Oak Ridge, TN 37831, USA*
[6] *Instituto de Astrofísica de Canarias, E-38200 La Laguna, Tenerife, Spain*
[7] *Departamento de Astrofísica, Universidad de La Laguna (ULL), E-38206 La Laguna, Tenerife, Spain*

Accepted, Received; in original form

ABSTRACT

We use Spitzer observations of the rich population of Asymptotic Giant Branch stars in the Large Magellanic Cloud (LMC) to test models describing the internal structure and nucleosynthesis of the most massive of these stars, i.e. those with initial mass above $\sim 4M_{\odot}$. To this aim, we compare Spitzer observations of LMC stars with the theoretical tracks of Asymptotic Giant Branch models, calculated with two of the most popular evolution codes, that are known to differ in particular for the treatment of convection.

Although the physical evolution of the two models are significantly different, the properties of dust formed in their winds are surprisingly similar, as is their position in the colour–colour (CCD) and colour–magnitude (CMD) diagrams obtained with the Spitzer bands. This model independent result allows us to select a well defined region in the $([3.6]-[4.5],[5.8]-[8.0])$ plane, populated by AGB stars experiencing Hot Bottom Burning, the progeny of stars with mass $M \sim 5.5M_{\odot}$. This result opens up an important test of the strength hot bottom burning using detailed near–IR (H and K bands) spectroscopic analysis of the oxygen–rich, high luminosity candidates found in the well defined region of the colour-colour plane. This test is possible because the two stellar evolution codes we use predict very different results for the surface chemistry, and the C/O ratio in particular, owing to their treatment of convection in the envelope and of convective boundaries during third dredge-up. The differences in surface chemistry are most apparent when the model stars reach the phase with the largest infrared emmission.

Key words: Stars: abundances – Stars: AGB and post-AGB. ISM: dust, extinction

1 INTRODUCTION

Stars in the mass range $0.8M_{\odot} \lesssim M \lesssim 8M_{\odot}$ evolve through the Asymptotic Giant Branch (AGB) (Becker & Iben 1980; Iben 1982; Iben & Renzini 1983; Lattanzio 1986). This evolutionary phase is characterized by a series of thermal pulses, caused by the unstable ignition of helium in a thin He–rich layer (Schwarzschild & Harm 1965, 1967). Although the timescale of the AGB is relatively short in comparison with the previous phases of core nuclear burning, the richest nucleosynthesis and the strongest mass loss occurs during this phase of evolution. This means that AGB stars are important for enriching the interstellar medium with the gas ejected from their surface layers and with the dust formed in their circumstellar envelopes.

Out of the stars that evolve through the AGB phase, those with initial masses above $\sim 4M_{\odot}$ exhibit an interesting behaviour and we will refer to these objects as massive AGB stars. First, massive AGB stars experience a second dredge-up, which leads to a large increase in the surface abundance of helium, which means that their ejecta is also strongly helium rich. Also, they experience Hot Bottom Burning (HBB), which occurs when the base of the convective mantle becomes sufficiently hot ($T_{\rm bce} > 30$MK)

to ignite proton–capture nucleosynthesis. The results of this nuclear processing are rapidly transported to the surface by convective currents, thus rendering these objects possible efficient polluters of gas processed by CNO burning and more generally, by advanced proton–capture nucleosynthesis.

The strength of Hot Bottom Burning is highly dependent on the description of convection, and especially so on the model used to determine the temperature gradient in regions unstable to convective motions. The extra luminosity from nuclear burning at the base of the convective envelope means that massive AGB stars deviate from the classic Paczyński (1970) relationship between core mass and luminosity (Renzini & Voli 1981; Blöcker & Schöenberner 1991)[1]. This was first shown by Renzini & Voli (1981) in the 1980s, who also noted that the deviation depends on the efficiency of the convective model used. D'Antona & Mazzitelli (1996) showed that HBB conditions can be easily obtained when the Full Spectrum of Turbulence (FST, Canuto & Mazzitelli 1991) description of convection is used instead of the traditional Mixing Length Theory (MLT). The study by Ventura & D'Antona (2005) importantly showed that convection modelling is by far the most important ingredient affecting the description of the evolution of massive AGB stars. Convection was shown to significantly affect the duration of the AGB phase, as well as the luminosity and the mass-loss rate of massive AGB stars.

Owing to our poor knowledge of the efficiency of HBB, the predictive power of the results of massive AGB stellar models is severely hampered. Models experiencing strong HBB contaminate the interstellar medium with gas that shows the signature of considerable CNO, Ne–Na and Mg–Al processing (Ventura & D'Antona 2008, 2009; Ventura et al. 2013) and dust, mainly in the form of silicate particles (Ventura et al. 2012a,b; Di Criscienzo et al. 2013; Ventura et al. 2014a). Conversely, in models with a less efficient HBB (and deeper third dredge-up, which mixes primary carbon, oxygen and magnesium to the surface), the oxygen and magnesium content of the ejecta are not as strongly modified with respect to the initial abundances (Karakas & Lattanzio 2007; Karakas 2010; Karakas & Lattanzio 2014). These models can even become carbon rich, where C/O $\geqslant 1$, at the end of the AGB phase, which means that solid carbon grains are the main dust component formed in their winds (Ferrarotti & Gail 2006).

All these uncertainties are a severe limitation to our understanding of the role played by massive AGB stars in a number of astrophysical contexts. A few examples of the importance of these objects include the possibility that they are the main actors in the formation of multiple populations in Globular Clusters (Ventura et al. 2001), that they have an important contribution to the dust present at high redshift (Valiante et al. 2009), and massive AGB stars are important for determining the chemical trends traced by stars in different parts of the Milky Way, as shown by models of galactic chemical evolution (Romano et al. 2010; Kobayashi et al. 2011).

These arguments stimulated us to start a comparative analysis, in an effort to significantly improve our understanding of the main physical properties of massive AGBs stars and particurly of the strength of HBB. The goal of this project is more than a mere comparison between results obtained with different stellar evolution models: we intend to test the robustness of the results obtained so far and to identify and suggest observations which could be relevant for discriminating among the different theoretical descriptions.

In this work we propose to use results from Spitzer observations of the AGB population of the Large Magellanic Cloud to allow a better understanding of their evolution properties. The LMC is an ideal laboratory for the study of AGB stars because they are relatively close ($d \sim 50$kpc, Feast 1999), with a low average reddening ($E(B-V) \sim 0.075$, Schlegel et al. 1998). A growing body of observational data, based on dedicated photometric surveys, has been recently made available to the community: the Magellanic Clouds Photometric Survey (MCPS, Zaritsky et al. 2004), the Two Micron All Sky Survey (2MASS, Skrutskie et al. 2006), the Deep Near Infrared Survey of the Southern Sky (DENIS, Epchtein et al. 1994), Surveying the Agents of a Galaxy's Evolution Survey (SAGE–LMC with the *Spitzer* telescope, Meixner et al. 2006), and *HERschel* Inventory of the Agents of Galaxy Evolution (HERITAGE, Meixner et al. 2010, 2013). Additional data allowed to reconstruct the Star Formation History (SFH) of the LMC (Harris & Zaritsky 2009; Weisz et al. 2013), and the age–metallicity relation (AMR, Carrera et al. 2008; Piatti & Geisler 2013). These studies outline that a burst in star formation occurred $\sim 80-100$Myr ago (Harris & Zaritsky 2009), indicating a significant population of massive AGB stars should be present in the LMC; these are the progeny of stars with initial mass $\sim 5-6 M_{\odot}$.

On the theoretical side, the recent investigations by Dell'Agli et al. (2014a, 2015) attempt an interpretation of the Spitzer observations of the LMC using evolution models of massive AGB stars, and a description of the dust formation mechanism in their winds. Dell'Agli et al. (2015) show that massive AGBs evolve into specific regions of the colour–colour and colour–magnitude planes obtained with the Spitzer bands, separated by the zones populated by dust–free AGB stars and dusty carbon stars. The agreement with the observations is remarkably good; however, the results obtained are extremely model dependent as the whole study used AGB models based on the FST description of convection.

Here we make a step forward. We compare the results by Dell'Agli et al. (2015) with those based on different models of massive AGB stars. Our scope is twofold: a) by comparing between models obtained with different prescriptions and codes, we aim to understand how stellar modelling uncertainties affect the dust formation process in the winds of massive AGB stars, and how that affects their position in the observational planes; and fix the uncertainties associated with the dust formation process in the winds of massive AGBs, and with the position occupied by these stars in the observational planes; b) we look for possible observations to be used to assess the strength of the HBB experienced by these sources.

The paper is organised as follows. The numerical and physical input to the AGB evolution models and the dust formation process are given in Section 2. In Section 3 we de-

[1] Garcia-Hernandez et al. (2009) observationally confirmed the extra HBB contribution to the luminosity in massive AGB stars in the Magellanic Clouds.

scribe the main physical features of the massive AGB models, whereas the properties of the dust formed in their winds is addressed in Section 4. In Section 5 we discuss the evolution of these stars in the observational planes obtained with the Spitzer bands.

2 NUMERICAL AND PHYSICAL INPUTS

The massive AGB star population in the LMC formed during the burst in the SFH that occurred $\sim 80-100$Myr ago (Harris & Zaritsky 2009). Half of the stars formed in that epoch have a metallicity $Z = 8 \times 10^{-3}$, with an additional lower metallicity component, with $Z = 10^{-3}$. Taking into account the evolution times of stars of intermediate mass, we deduce that most of the massive AGB stars observed today in the LMC are the descendants of stars with initial mass $M \sim 5.5 M_{\odot}$. Based on these arguments, we will focus in the following on stellar models of mass $M = 5.5 M_{\odot}$ and metallicity $Z = 8 \times 10^{-3}$. We are interested to the behaviour of dusty, obscured, oxygen–rich sources and for this reason we neglect the lower-Z component. These low-metallicity objects have a smaller silicon abundance, which leads to lower dust production rates (Ventura et al. 2014a) during the oxygen–rich phase.

2.1 Stellar evolution models

The models presented in this work were calculated with the ATON code (Ventura et al. 1998) and with the Monash version of the Mount Stromlo Stellar Structure Program (Frost & Lattanzio 1996). We will refer to these models as the ATON and MONASH models, respectively.

The interested reader is referred to the papers by Ventura et al. (2013) and Karakas (2010) for a detailed discussion of the numerical and physical inputs used to calculate the evolutionary sequences and for an exhaustive description of the chemical and physical properties of the AGB evolution of these stars. Both models were evolved until the almost complete loss of the convective envelope.

The main differences between the two sets of models is in the treatment of convection and the description of mass loss. In the ATON code the convective instability is described by means of the FST model, whereas in the MONASH case the traditional MLT treatment is used. The mass-loss rate in the ATON case is determined via the Blöcker (1995) treatment, whereas the MONASH models adopt the Vassiliadis & Wood (1993) mass-loss prescription.

2.2 Dust formation in the winds of AGB stars

The growth of dust particles is calculated with a simple model for the stellar wind. This is based on the pioneering explorations by the Heidelberg group (Gail & Sedlmayr 1985, 1999; Ferrarotti & Gail 2001, 2002, 2006; Zhukovska et al. 2008) and was extensively used in previous works by our group (Ventura et al. 2012a,b; Di Criscienzo et al. 2013; Ventura et al. 2014a), as also in works of other researchers (Nanni et al. 2013a,b, 2014).

The outflow is assumed to expand symmetrically from the stellar surface, with an initial velocity of 1 km s^{-1}. The description of the wind is given by solving two differential equations, which describe the radial variation of the gas velocity and of the optical depth, τ:

$$v \frac{dv}{dr} = -\frac{GM_*}{r^2}(1-\Gamma), \tag{1}$$

$$\frac{d\tau}{dr} = -k\rho \left(\frac{R_*}{r}\right)^2, \tag{2}$$

where M_* and R_* are the stellar mass and luminosity, ρ is the density of the gas, k is the extinction coefficient and Γ is given by the expression

$$\Gamma = \frac{kL_*}{4\pi c G M_*}, \tag{3}$$

with L_* indicating the luminosity of the star.

The above equations are completed by the mass conservation equation, for density, and the relationship governing the radial variation of temperature as a function of the effective temperature of the star:

$$\rho = \frac{\dot{M}}{4\pi r^2 v}, \tag{4}$$

$$T^4 = \frac{1}{2} T_{eff}^4 \left[1 - \sqrt{1 - \left(\frac{R_*}{r}\right)^2}\right] + \frac{3}{2}\tau. \tag{5}$$

Γ is the key quantity for the dynamics of the wind: the expanding gas can be accelerated only when the condition $\Gamma > 1$ is reached. Eq. 3 shows that the acceleration of the wind is favoured by large luminosities, as a consequence of the large radiation pressure determined by large values of L_*. A high k can also produce a large acceleration of the wind. The value of k depends on the number density and the size of the dust particles of the various species formed. The growth of the dimension of the various dust particles forming in the wind is described by means of additional equations, giving the growth rate of each species as a function of the local values of density and temperature and of the surface abundance of the elements relevant for the formation of each dust species.

In oxygen–rich environments (C/O below unity) we consider the formation of alumina dust (Al_2O_3), silicates and solid iron. The relevant elements for the formation of these dust species are aluminium, silicon and iron. When $C/O > 1$ we follow the formation of solid carbon grains, silicon carbide and solid iron; in this case the key–elements are carbon, silicon and iron.

The whole set of equations describing the dust formation process is described and commented in details in Ventura et al. (2012a,b); Di Criscienzo et al. (2013); Ventura et al. (2014a).

2.3 Synthetic spectra

For each point of the evolutionary sequence we compute the magnitudes in the various Spitzer bands by calculating the synthetic spectra. This is done in two steps:

• The results from stellar evolution modelling, particularly the values of mass, luminosity, effective temperature, mass-loss rate and surface chemical composition, are used to find out the dust species formed in the wind, the size of the dust grains and the optical depth (here we use the value at 10μm, τ_{10}).

• By means of the code DUSTY (Nenkova et al. 1999) we calculate the synthetic spectra of each selected point along the evolutionary sequence; the magnitudes in the various bands are obtained by convolution with the appropriate transmission curves.

The code DUSTY needs as input parameters the effective temperature of the star, the radial profile of the density of the gas and the dust composition of the wind, in terms of the percentage of the various species present and of the the size of the dust particles formed. All these quantities are known based on the results of stellar evolution and of the description of the wind.

In the recent investigation by Dell'Agli et al. (2015) we give the details on the way DUSTY is used to determine the synthetic spectra both of oxygen–rich stars and of carbon stars.

3 THE ROLE OF HOT BOTTOM BURNING IN THE EVOLUTION OF MASSIVE AGBS

The main features of the evolution of stars of low and intermediate mass along the AGB phase have been thoroughly discussed in the literature, together with the uncertainties associated to the various physical inputs adopted. We address the interested reader to the exhaustive reviews on this argument by Herwig (2005) and Karakas & Lattanzio (2014).

In massive AGB models, two mechanisms may potentially alter the surface chemical composition: Hot Bottom Burning and Third Dredge Up (TDU). In the first case the surface chemistry changes according to the equilibrium abundances of proton–capture nucleosynthesis, which in turn depends on the temperature at the base of the convective envelope. The ignition of HBB determines the decrease in the surface carbon in favour of nitrogen; when the HBB is strong (with temperatures above ~ 70 MK) oxygen and magnesium are destroyed and sodium and aluminium are produced. TDU is the inward penetration of the surface convection after each thermal pulse down to layers contaminated by 3α nucleosynthesis. The main modification of the surface chemical composition by TDU is the gradual increase in the carbon content, although both oxygen and magnesium can also be dredged up as a consequence of partial helium burning (Herwig 2000; Karakas & Lattanzio 2003).

The ATON and MONASH codes have been written and developed independently from each other; they differ in the numerical structure and in the description of some physical mechanisms relevant for the evolution on the AGB, primarily convection and mass loss. We therefore expect that the differences among the results obtained provide a valuable indication of the uncertainties affecting the evolution of massive AGB stars.

To this aim, we compare the results concerning the evolution of two models of initial mass $M = 5.5M_{\odot}$ and metallicity $Z = 8 \times 10^{-3}$. The reason behind this choice is partly that this mass is within the range of masses experiencing HBB; additionally, on the basis of the arguments presented in section 2, we know that in the LMC this is the typical mass evolving today as a massive AGB star.

Fig. 1 shows the temporal variation of the main physical and chemical quantities of the ATON and MONASH models during the AGB phase. We show the evolution of the luminosity, the mass-loss rate, the effective temperature, and the surface C/O ratio.

Common features in the behaviour of the two sequences are the gradual increase in the luminosity L, characterizing the first part of the AGB evolution, due to an increase in the core mass, and the decline of L in the final AGB phases, a consequence of the progressive shutting down of HBB. The rate at which mass loss occurs follows a similar trend, reaching the highest value in the middle of the AGB phase. The surface regions become cooler and cooler as the total mass of the star diminishes: the effective temperature decreases from the initial value of $T_{\rm eff} \sim 3600$K to $T_{\rm eff} \sim 2800$K in the latest stages.

Other than these similarities, we see from Fig. 1 that the two models exhibit considerable differences.

First, the ATON models evolve to larger luminosities. The $5.5M_{\odot}$ ATON model reaches a maximum luminosity of $\sim 6 \times 10^4 L_{\odot}$, whereas the corresponding MONASH model reaches $L \sim 4 \times 10^4 L_{\odot}$. To show that the difference between the two models is intrinsic, we also show the evolution of the ATON $5M_{\odot}$ model, which, though evolving on a core of smaller mass, reaches a higher luminosity ($L \sim 5 \times 10^4 L_{\odot}$) than the MONASH case. This difference is not surprising, considering the different description of convection adopted in the two cases. Ventura & D'Antona (2005) clearly showed that the use of the FST model leads to stronger HBB conditions and to higher luminosities. We note in Fig. 1 that in the ATON case, owing to an early ignition of HBB, the luminosity starts to increase very fast since the early AGB phases, at odds with the MONASH model, in which the increase in the overall flux is more gradual.

The rate at which mass is lost reflects the differences among the luminosities. ATON models experience larger mass-loss rates, which reach $\dot{M} \sim 10^{-4} M_{\odot}/yr$ in the phase of maximum luminosity. The MONASH model experience a weaker mass loss: $\dot{M} < 5 \times 10^{-5} M_{\odot}/yr$ during the whole AGB phase. The mass-loss rate experienced by the ATON models reflects the strong variation in the luminosity. This is because the Blöcker (1995) description of mass loss is much more sensitive to luminosity than the Vassiliadis & Wood (1993) recipe.

The strong mass-loss rates experienced by the ATON models has an important consequence for the duration of the AGB phase. The duration of the AGB phase in the MONASH model is $\sim 4 \times 10^5$ yr, a factor of 2.6 longer than the ATON case, which has a duration of less than $\sim 1.5 \times 10^5$ yr.

The evolution of the surface chemistry also shows considerable differences between the two models. Here we focus on the C/O ratio, a valuable indicator of the strength of HBB and of the extent of the Third Dredge–Up. In the ATON models (see Fig. 1) HBB favours a strong depletion of the surface C/O after a few 10^4yr, owing to the destruction of the surface carbon, via proton fusion. The C/O ratio remains below ~ 0.05 for the rest of the AGB evolution,

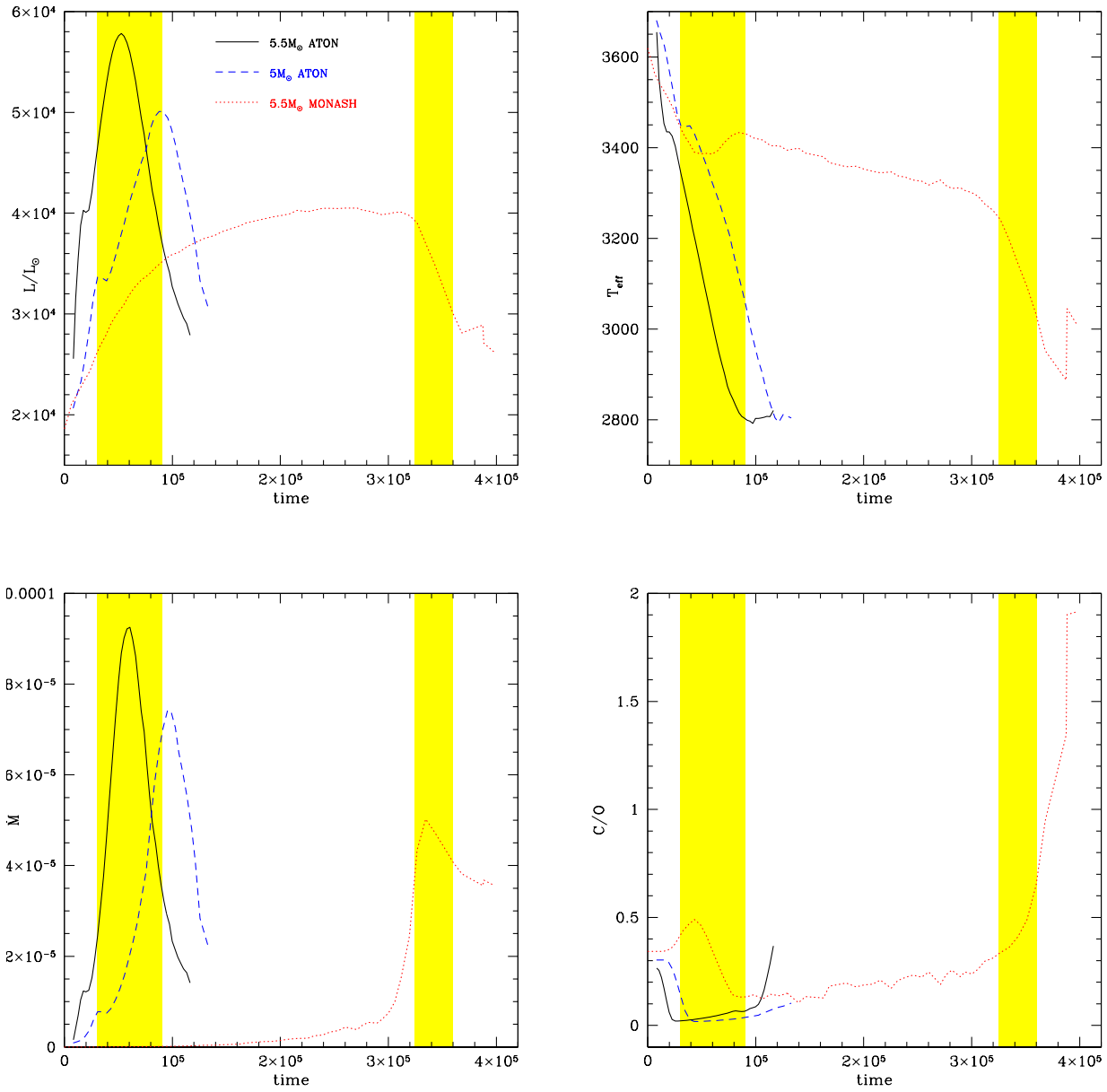

Figure 1. The evolution of luminosity (left–top panel), effective temperature (right–top), mass-loss rate (left–bottom) and surface C/O ratio (right–bottom) of massive AGB models calculated with the the ATON and MONASH stellar evolution codes. Times are counted from the beginning of the AGB phase. The shaded regions indicate the phase of highest mass loss rate and strongest infrared emission for the ATON and MONASH models of initial mass $5.5M_{\odot}$.

because the carbon transported to the surface by TDU is immediately destroyed by HBB. Only in the very final evolutionary phases, when HBB is practically quenched by the general cooling determined by the gradual loss of the convective envelope, the surface C/O increases. The MONASH model experiences a weaker HBB. In the competition between TDU and HBB, the latter prevails only in the period $2-4\times10^5$yr, when the C/O ratio drops to 0.15. Following HBB shutting down, the C/O ratio gradually increases and in the very final phases the model becomes carbon rich.

4 DUST FROM MASSIVE AGB STARS

A common feature of the ATON and MONASH models is that for most of the AGB evolution massive AGB stars

evolve as oxygen–rich stars. Only during the final few thermal pulses does the MONASH model reach the carbon star stage.

The amount of dust formed in the winds of oxygen–rich AGBs is affected by the strength of the HBB experienced (Ventura et al. 2012b): models suffering stronger HBB evolve at larger luminosities, loose their envelope with a higher rate, which, in turn, favours the growth of dust particles in the wind. Based on the differences between the physical properties of the ATON and MONASH models outlined in the previous section, we focus now on the description of how these reflect into the dust formation process expected in the two cases.

In oxygen–rich environments the most stable species is alumina dust, which forms at temperatures $T \sim 1500$K, at a distance from the surface of the star of the order of $\sim 2-3$ stellar radii (Dell'Agli et al. 2014b). Additional species forming are silicates, in the form of olivine, pyroxene and quartz (Ferrarotti & Gail 2006). The silicates are less stable than alumina dust and only form in more external regions ($d \sim 7-10R_*$), at temperatures $T \sim 1100$K. Solid iron is even less stable, thus it forms in even more external and cooler layers, in smaller quantities.

Alumina dust is transparent to electromagnetic radiation. This means that the wind is barely (or not at all) accelerated by the formation of Al_2O_3 grains. Therefore the wind enters the region of silicates formation with a velocity close to the initial velocity. The main consequence is that the formation of silicates is not affected by the amount of alumina dust formed.

The presence of silicate grains has a much stronger influence on the dynamics of the wind: the large values of the extinction coefficient, k, provokes a strong acceleration of the gas particles, owing to the increase of Γ (see Eqs. 1 and 3 in Section 2 and the discussion on the role of Γ on the acceleration of the wind).

Fig. 2 shows the evolution of the size of the various dust particles formed during the AGB phase for the ATON and MONASH models, discussed in the previous section. The ATON $5M_{\odot}$ is not shown here, as we have seen that it shares many similar properties to the more massive models. For clarity we show only the size of the three most abundant species formed, i.e., olivine, pyroxene and alumina dust. We see that the dust properties of the two models during the highest luminosity phase are very similar. In both cases we find that the central star is surrounded by an optically thick dust layer, dominated by olivine grains, with size slightly above 0.1μm and pyroxene particles of smaller size, with typical dimension $\sim 0.06-0.07\mu$m. The only differences found is in the properties of the alumina dust formed. In the ATON model the Al_2O_3 grains reach a larger size ($\sim 0.05\mu$m) compared to the MONASH case ($\sim 0.03-0.04\mu$m). The reason for the larger grain growth in the ATON models is explained below.

This result is at first surprising, given the differences in the physical AGB evolution of the two models. To understand the reason for the similarities found, we need to analyze the dynamics of the wind and the coupling with the dust formation process.

To this aim, we show in Fig. 3 the radial variation of the thermodynamic quantities, including the size of alumina dust and olivine grains formed, the velocity of the wind and of Γ. This figure refers to the ATON and MONASH models during the respective phases of highest mass loss rate.

In the previous section we have seen that the ATON model experiences a higher mass-loss rate. This favours a higher density in the wind (see Eq. 4) and a more efficient formation of dust, owing to a larger availability of gas molecules in the wind. On the other hand the FST models are more luminous and evolve on more expanded configurations. This has no effect on the temperature stratification, which depends on r/R_* (see Eq. 5), but it affects the density, which, based on Eq. 4, scales as $1/r^2$. This effect partly compensates for the higher $\dot{M}$ of the ATON model, decreasing the density gap with the MONASH case. The production of alumina dust is higher in the ATON case, the size of the Al_2O_3 grains growing faster as the wind expands outwards.

As discussed above, formation of alumina dust is not sufficient to accelerate the wind. The profile of Γ remains practically flat (we note only a modest increase of Γ in the ATON case, but still with $\Gamma < 0.1$) in the whole region internal to the zone where the formation of silicates occurs.

When entering the region where formation of silicates begins, the ATON wind is denser than in the MONASH case but the difference is below a factor ~ 2, as explained above. Unlike with alumina dust, the formation of silicates provokes a strong acceleration of the wind, owing to the effects of radiation pressure. This can be clearly seen in the increase in the values of velocity and of Γ, accompanying the increase in the size of olivine grains. The acceleration experienced by the MONASH wind is smaller but this indirectly favours the formation of silicates, because the condensation zone is wider. This is the reason why the size reached by olivine grains in the MONASH model is only slightly smaller than in the ATON case.

The results shown in Fig. 2 are of extreme importance for the studies focused on dust production around massive AGB stars. Despite the fact that our comparison identified significant differences in several physics aspects of AGB evolution between the ATON and MONASH models, the results in terms of the dust formation process are much more homogeneous. During the phase when the models reach the highest rate of mass loss, they are both surrounded by two dusty layers: an internal region, populated by alumina dust grains (with typical dimension of $\sim 0.05\mu$m), and a more external zone, with silicates grains of $\sim 0.1\mu$m size. These results are rather robust at the metallicity of the LMC ($Z = 8 \times 10^{-3}$) and independent of the details of AGB modelling.

This is a welcome result for the reliability of this kind of investigation. The main criticism put forward for this description is that the mass-loss rate is assumed as a boundary condition, rather than being deduced on the basis of the amount of dust formed. However, these results confirm that for massive AGB stars the dust formation process is not strongly dependent on the mass-loss rate assumed.

In terms of the overall dust mass produced by these stars, we find that models experiencing strong HBB produce more silicates and alumina dust. In the ATON case the mass of silicates and of Al_2O_3 produced are, respectively, $M_{sil} = 3 \times 10^{-3} M_{\odot}$ and $M_{Al_2O_3} = 2 \times 10^{-4} M_{\odot}$, whereas the MONASH model gives $M_{sil} = 1.7 \times 10^{-3} M_{\odot}$ and $M_{Al_2O_3} = 4.2 \times 10^{-5} M_{\odot}$. In the latter case we also have production of carbon dust, with mass $M_C = 4.5 \times 10^{-4} M_{\odot}$. The reason for this differences can be understood based on

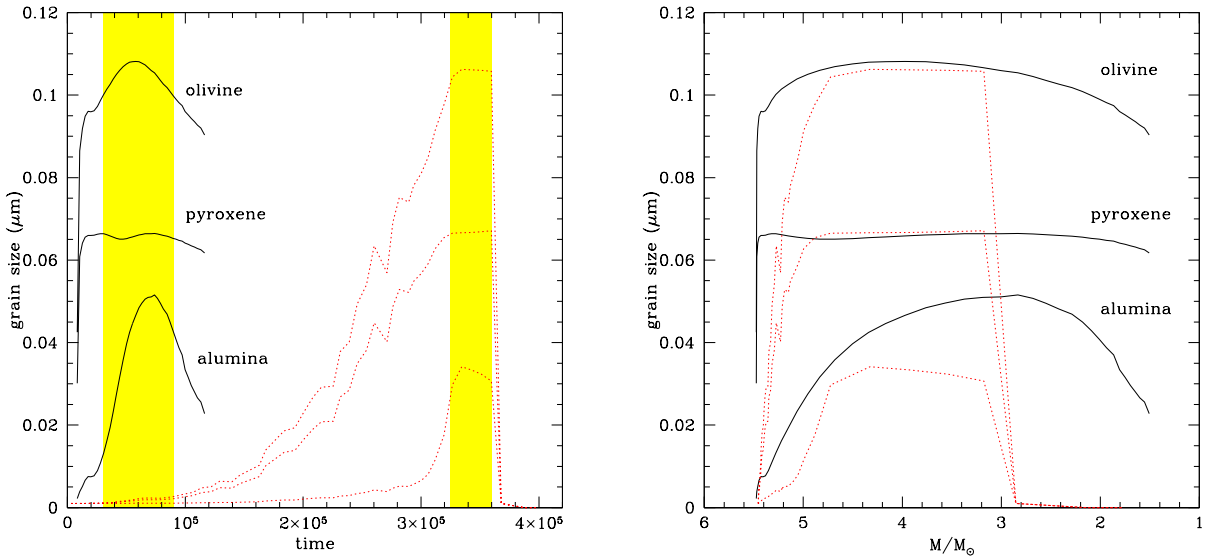

Figure 2. Evolution of the size of the olivine, pyroxene and alumina dust grains formed in the wind of the $5.5M_{\odot}$ models shown in Fig. 1 during the AGB phase. The variation of the grain size as a function of the time counted from the beginning of the AGB phase (left panel) and of the current mass of the star (right panel) are shown. The two sets of tracks indicate results from ATON (solid) and MONASH (dotted) codes. The shaded regions in the left panel have the same meaning as in Fig. 1.

the right panel of Fig. 2. In the ATON case silicate particles are produced during the whole phase of mass loss, whereas in the MONASH model this is restricted to the phases when the rate of mass loss attains its largest values: the production of silicates is modest in the initial AGB phases and is null in the final part of the evolution, when the C/O ratio exceeds unity.

A definitive confirm to these findings can be obtained only on the basis of radiation-hydrodynamical models. The analysis by Höfner (2008) and Bladh & Höfner (2012) confirmed that iron–free silicates, particularly Mg_2SiO_4, are viable wind–drivers in O–rich stars, owing to the significant contribution of scattering to their extinction coefficients. This self–consistent method, applied to the winds of stars of smaller mass ($M \sim 1M_{\odot}$) and lower luminosity ($L < 10^4 L_{\odot}$) than those of interest here, showed that silicate particles of size in the range $\sim 0.1 \; - 1\mu$m can potentially accelerate the wind. A similar approach is needed for the massive AGB stars examined in this work to assess whether the typical dimension of $\sim 0.12\mu$m, found in our case, is sufficient to favour radiative acceleration of the wind.

5 EVOLUTIONARY PROPERTIES AND SPITZER COLOURS OF AGB STARS

In a recent investigation, aimed at interpreting the Spitzer observations of obscured AGB stars in the LMC, Dell'Agli et al. (2015) made a characterization of the AGB population in terms of age, initial mass and dust properties. The main result of this study was that carbon and oxygen–rich stars with large infrared emission populate two distinct regions in the colour–colour ([3.6] − [4.5], [5.8] − [8.0]) plane, enclosed within the two boxes shown in the left panel of Fig. 4; the two groups of stars were defined, respectively, OCS (obscured carbon stars) and HBBS (stars experiencing Hot Bottom Burning). OCS, with solid carbon and silicon carbide (SiC) particles in their wind, evolve along a diagonal band, extending from [3.6] − [4.5] ∼ 0.2 to [3.6] − [4.5] ∼ 3. HBBS, surrounded by alumina and silicates grains, populate the zone on the upper side of the diagram, centred at ([3.6] − [4.5], [5.8] − [8.0]) ∼ (0.3, 0.7).

A less evident separation between the two groups of stars is present in the colour–magnitude ([3.6] − [8.0], [8.0]) plane: in this case OCS evolve along a diagonal band, extending to [3.6] − [8.0] ∼ 6, whereas HBBS define a more vertical sequence, with colours [3.6] − [8.0] < 2 (see Fig. 11 and Fig. 12 in Dell'Agli et al. 2015).

The interpretation by Dell'Agli et al. (2015) is largely consistent with samples of spectroscopically confirmed (e.g., with Spitzer spectra) AGB stars. However, different results and/or interpretations may be found among different authors in the literature. In particular, Riebel et al. (2012), based on best-fit GRAMS models, suggest that ∼ 25% of stars in the HBBS region are carbon stars. Turning to OCS, interpreted by Dell'Agli et al. (2015) as a sample entirely composed by carbon stars, preliminary analysis based on red optical spectra (Boyer et al. 2015, in preparation) may indicate that a few O-rich sources belong to the OCS group. These differences stress the need either for an improvement in the description of dust formation in the winds of AGBs, and/or a refinement of the classifcation of AGBs based on red optical spectra.

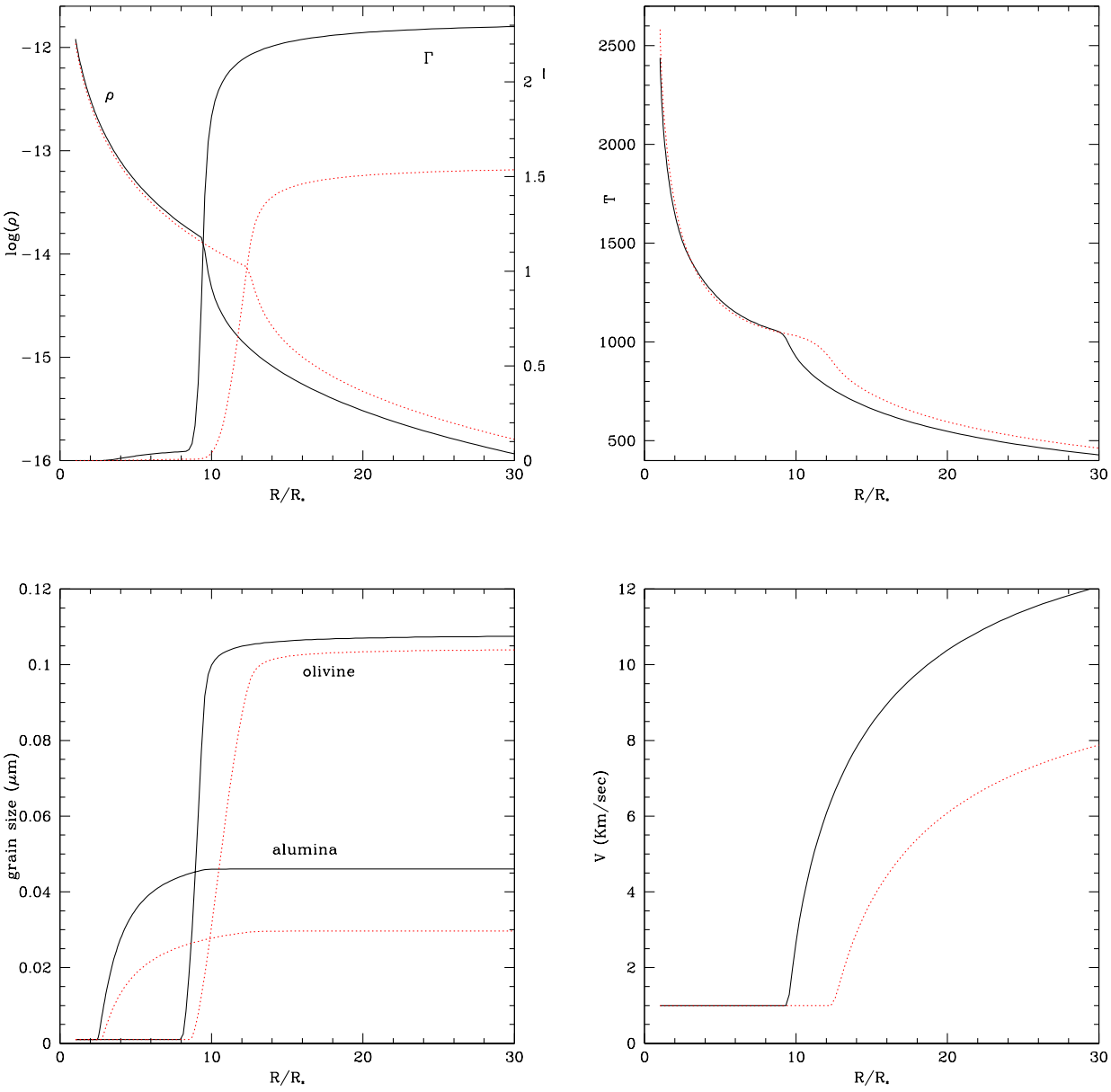

Figure 3. The structure of the wind of the ATON (solid) and MONASH (dotted) models during the phase of highest mass loss rate. The quantities shown are the radial profiles of density and Γ (left–top panel), temperature (right–top), size of the grains formed (left–bottom) and velocity of gas (right–bottom). Distances are measured from the centre of the star and are expressed in units of stellar radii.

Understanding the reasons for these discrepancies is far beyond the scope of this work. However, in the following we will focus on stars in the HBBS region confirmed to be oxygen–rich.

The ATON model is a typical example of a massive AGB star, belonging to the HBBS sample. The comparison between the tracks of the ATON and MONASH models, shown in Fig. 4, shows a remarkable similarity: during the phases with the largest infrared emission (corresponding to the shaded regions in Fig. 1) the two tracks are practically overimposed in the colour–colour plane, a consequence of the similarities in the dust properties. The only difference is in the very final AGB phases, when the MONASH model reaches a C/O ratio greater than one and evolves to the OCS sequence in the colour–colour plane, whereas the track of the ATON case stays in the HBBS region.

This is a welcome result, adding more robustness to the conclusion by Dell'Agli et al. (2015). It shows that massive

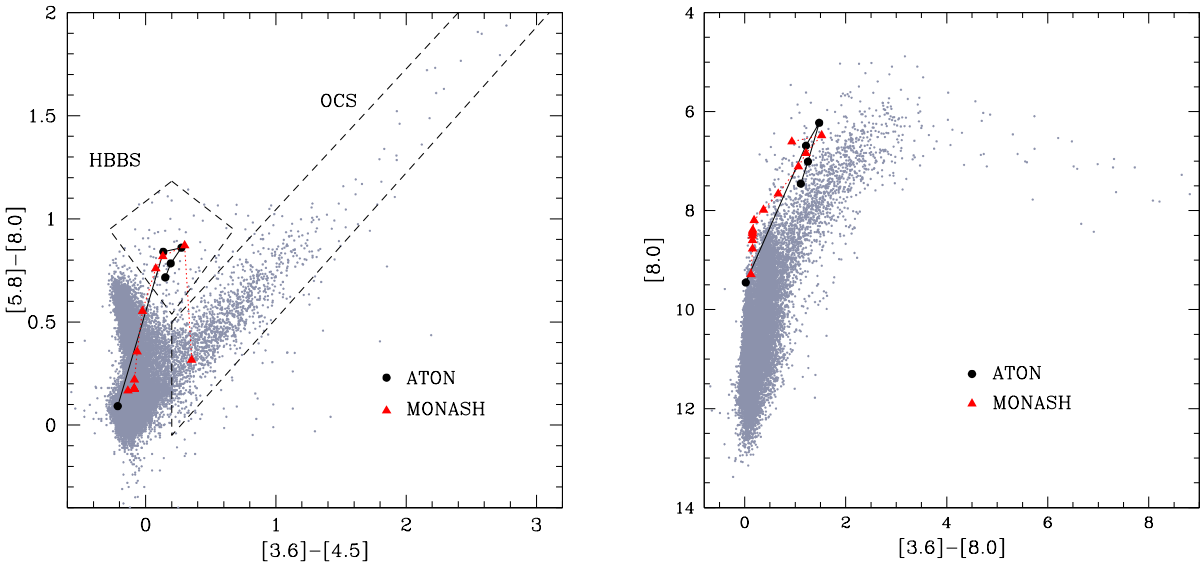

Figure 4. The evolution of the ATON and MONASH models of initial mass $5.5 M_{\odot}$ and metallicity $Z = 8 \times 10^{-3}$ in the colour–colour ([3.6] − [4.5], [5.8] − [8.0]) plane (left panel) and in the colour–magnitude ([3.6] − [8.0], [8.0]) diagram. The points are taken at time intervals of 3×10^4yr. Grey dots indicate the sample of AGBs in the LMC by Riebel et al. (2012). The two boxes enclose the regions of the colour–colour plane where obscured carbon stars (OCS) and oxygen–rich stars (HBBS) are expected to evolve, based on the present analysis and on the works by Dell'Agli et al. (2014a, 2015).

AGB stars, during the phase of highest mass loss rate, evolve to the HBBS region and that this result is independent of the details of AGB modelling. Dell'Agli et al. (2015) suggested that only stars experiencing strong HBB would populate this region of the colour–colour plane, whereas here we reach a more general conclusion: all massive AGB stars of the metal–rich component in the LMC will evolve into this zone of the diagram.

We return to the main goal of this investigation, i.e., understanding whether the large sample of AGB stars in the LMC can be used as a laboratory to test the evolution models of massive AGB stars and to constrain the strength of the Hot Bottom Burning experienced. The results found here rule out the possibility that this task can be accomplished on the basis of pure photometric arguments, because the relevant models evolve to very similar colours, independently of the details of convection modelling. As shown in the right panel of Fig. 4, in the colour–magnitude diagram the ATON model reaches lower [8.0] magnitudes ([8.0] $\sim$ 5.7) compared to the MONASH case ([8.0] $\sim$ 6.2); however, the statistics in that region of the diagram does not allow to use this information as a valuable discriminator between the two descriptions.

The number counts would also be of little help here: despite the overall AGB phase of the MONASH model is longer, the duration of the phase with the largest infrared emission are similar in the two cases (compare the horizontal extension of the shaded regions in Fig. 1), thus preventing any possibility of discriminating based on the number of stars observed in the HBBS region. In the MONASH case we expect a larger population of AGBs in the region of the colour–colour plane clustering around [3.6] − [4.5] $\sim$ 0, where no–dusty, oxygen–rich stars evolve. However, this argument cannot be used to discriminate among the models: Dell'Agli et al. (2015) showed that the vast majority of stars in that region (see Fig. 15 in Dell'Agli et al. (2015)) are the progeny of low–metallicity stars of mass $1 - 2 M_{\odot}$ (see Fig. 15 in Dell'Agli et al. (2015)). The fraction of massive AGBs present in that region is below 2%, so on number counts alone it will be difficult to distinguish between the ATON and MONASH prescriptions. A better test of the models is a spectrscopic analysis of the massive AGB stars, using the stars found from our model independent results for the colour-colour plane.

The predictions of the two models show up significant differences in the dust production rate (DPR) expected from oxygen–rich and carbon stars. Schneider et al. (2014) used ATON models to derive an overall DPR from AGBs of $\sim 4.5 \times 10^{-5} M_{\odot}/yr$, with a contribution from carbon and oxygen–rich stars of, respectively, $\sim 4 \times 10^{-5} M_{\odot}/yr$ and $\sim 5 \times 10^{-6} M_{\odot}/yr$. Based on the MONASH models we expect a smaller relative contribution from oxygen–rich stars. This is because massive AGB stars are the dominant contributors to the overall silicate DPR and the MONASH model is predicted to produce less silicates compared to the ATON models and to provide a contribution to the overall carbon dust produced, not present in the ATON case.

While the ATON result for the DPR from oxygen–rich AGBs is in reasonable agreement with Riebel et al. (2012) and Matsuura et al. (2009), the studies from Srinivasan et al.

(2009) and Boyer et al. (2012) point in favour of MONASH modelling: however, the DPRs in the LMC are estimated using different assumptions about grain properties, resulting in factors of at least $2-4$ uncertainties, so it is difficult to make direct comparisons. A reliable estimate of the DPR from AGB stars appears as a future, promising indicator of the evolution properties of massive AGB stars.

Despite the similarities in the photometric properties, the surface chemistry of the ATON and MONASH model during the phase characterised by the large infrared emission (indicated with a shaded region in Fig. 1) is considerably different. This can be clearly seen in the right–bottom panel of Fig. 1, showing the evolution of the surface C/O ratio. In the ATON case the chemistry is entirely dominated by the effects of HBB: the C/O ratio is extremely small, with $C/O < 0.05$, owing to the destruction of the surface carbon via proton fusion. Conversely, in the MONASH model, the behaviour of the surface chemistry is affected by both the effects of Third Dredge Up and HBB: in this case the C/O ratio at the surface of the star is much larger, with $C/O \sim 0.5$, a factor of 10 higher.

We reach the conclusion that the spectroscopic analysis of the stars populating the region enclosed within the HBBS box in the colour–colour ([3.6] − [4.5], [5.8] − [8.0]) plane (left panel of Fig. 4), introduced by Dell'Agli et al. (2015), will be a powerful indicator of the strength of HBB suffered by massive AGB stars with a metallicity of $Z = 8 \times 10^{-3}$. The results obtained here are a robust confirm that these stars are massive AGB stars, surrounded by a thick layer of silicate dust. If the HBB experienced by these stars is strong, their surface chemistry will reflect the equilibria of proton capture nucleosynthesis, with a C/O ratio below 0.05; there is no way to escape from this conclusion, because the stars populating the HBBS region are expected to be in the phases of strongest Hot Bottom Burning. On the contrary, a value of $C/O \sim 0.5$ would point in favour of a less efficient convection in the envelope, and of a soft HBB.

McSaveney et al. (2007) presented high–dispersion, near–IR spectra of highly evolved AGB stars in the SMC and LMC. For a couple of LMC stars the CNO abundances derived showed–up the signature of HBB, with nitrogen enhancement and carbon deficiency. In particular, they measured the C/O ratios in two LMC-HBB AGBs (HV 2576 and NGC 1866 #4), obtaining C/O=0.05 and 0.04 in HV 2576 and NGC 1866 #4, respectively. However, near-IR (H and K bands), high-resolution (R$> 20,000$) spectroscopic observations, extended to the O-rich stars in the HBBS sample, would be needed to confirm the earlier McSaveney et al. (2007) results and to definitively fix the strength of the HBB experienced by these stars.

6 CONCLUSIONS

We use the large sample of AGB stars in the LMC to constrain the evolutionary properties of massive AGB stars, i.e., stars with initial mass $M > 4M_{\odot}$, that are know to experience Hot Bottom Burning at the base of their convective mantle. The main goal is to draw information on the strength of the HBB experienced, via a comparison between theoretical models and observations.

To this aim, we compare results from two independent research groups involved in AGB studies, whose models of massive AGB stars are known to differ in the efficiency of the convection modelling, and consequently in the HBB experienced.

The dust formation process in the winds of these stars is found to be essentially independent of the details of AGB modelling. During the phases when the stars evolve at the highest luminosity, a common behaviour of the different models is the formation of alumina dust and silicates grains. The former species is more stable and form in a more internal region, with the grain size distribution peaked at $\sim 0.05\mu$m, partly dependent on the AGB model used. Silicate particles of $\sim 0.12\mu$m size form in a more external region; owing to their large extinction coefficients, this dust species favour the acceleration of the wind, up to velocities of the order of $10-15$ km s^{-1}.

Owing to the similarity in the dust composition surrounding the stars, the infrared colours expected are also practically independent of AGB modelling.

This result is in agreement with recent investigations and offer the opportunity of selecting a well defined region in the colour–colour ([3.6]−[4.5], [5.8]−[8.0]) plane where massive AGBs, experiencing Hot Bottom Burning, evolve. More important, this finding indicates the possibility of an observational test of the efficiency of the Hot Bottom Burning experienced by AGBs, at least at the metallicity typical of young LMC stars. This analysis will be possible because we have shown that the surface chemical composition of massive AGB stars during the phase with the highest infrared emission is extremely sensitive to convection modelling: we suggest that a near-IR (H and K bands) spectroscopic follow–up of the stars identified as massive AGBs based on their position on the aforementioned plane would provide a clear and straight indication of the strength of HBB experienced.

ACKNOWLEDGMENTS

P.V. was supported by PRIN MIUR 2011 "The Chemical and Dynamical Evolution of the Milky Way and Local Group Galaxies" (PI: F. Matteucci), prot. 2010LY5N2T. A.I.K. was supported through an Australian Research Council Future Fellowship (FT110100475). D.A.G.H. acknowledges support provided by the Spanish Ministry of Economy and Competitiveness under grant AYA-2011-27754. R.S. acknowledges funding from the European Research Council under the European Unions Seventh Framework Programme (FP/2007- 2013)/ERC Grant Agreement n. 306476.

REFERENCES

Allard F., Homeier D., Freytag B., 2012, Philosophical Transactions of the Royal Society A: Mathematical, Physical and Engineering Sciences, vol. 370, issue 1968, pp. 2765-2777
Becker S. A., Iben I. Jr. 1980, ApJ, 237, 111
Bladh S., Höfner S. 2012, A&A, 546, 76
Blöcker T., 1995, A&A, 297, 727
Blöcker T., Schöenberner D., 1991, A&A, 244, L43
Boyer M. L., Srinivasan S., Riebel D., McDonald I., van

Loon J. Th., Clayton G. C., Gordon K. D., Meixner M., Sargent B. A., Sloan G. C., 2012, ApJ, 748, 40
Canuto V. M. C., Mazzitelli I., 1991, ApJ, 370, 295
Carrera R., Gallart C., Hardy E., Aparicio A., Zinn R., 2008, AJ, 135, 836
D'Antona,F., Mazzitelli I. 1996, ApJ, 470, 1093
Dell'Agli F., Ventura P., Garcia-Hernandez D. A., Schneider R., Di Criscienzo M., Brocato E., D'Antona F., Rossi C. 2014a, MNRAS, 442, L38
Dell'Agli F., Garca-Hernndez D. A., Rossi C., Ventura P., Di Criscienzo M., Schneider R. 2014b, MNRAS, 441, 1115
Dell'Agli F., Ventura P., Schneider R., Di Criscienzo M., Garcia-Hernandez D. A., Rossi C., Brocato E. 2015, MNRAS, 447, 2992
Di Criscienzo M., Dell'Agli F., Ventura P., Schneider R., Valiante R., La Franca F., Rossi C., Gallerani S., Maiolino, R., 2013, MNRAS, 433, 313
Epchtein N. et al., 1994, AP&SS, 217, 3
Feast M., 1999, PASP, 111, 775
Ferrarotti A. D., Gail H. P., 2001, A&A, 371, 133
Ferrarotti A. D., Gail H. P., 2002, A&A, 382, 256
Ferrarotti A. D., Gail H. P., 2006, A&A, 553, 576
Frost C. A., Lattanzio J. C. 1996, ApJ, 473, 383
Gail H. P., Sedlmayr E., 1985, A&A, 148, 183
Gail H. P., Sedlmayr E., 1999, A&A, 347, 594
Garca-Hernndez, D. A., Manchado, A., Lambert, D. L. et al. 2009, ApJ, 705, L31
Grevesse N., Sauval A. J, 1998, SSrv, 85, 161
Harris J. & Zaritsky D. 2009, ApJ, 138, 1243
Herwig F. 2005, ARA&A, 43, 435
Höfner S. 2008, A&A, 491, L1
Herwig F., 2000, A&A, 360, 952
Herwig F., 2005, AR&A, 43, 435
Iben I. Jr. 1982, ApJ, 260, 821
Iben I. Jr., Renzini A. 1983, ARA&A 21, 271
Lattanzio J. C. 1986, ApJ, 311, 708
Karakas A., Lattanzio J. C. 2003, PASA, 20, 393
Karakas A., Lattanzio J. C. 2007, PASA, 24, 103
Karakas A. I. 2010, MNRAS, 403, 1413
Karakas A. I. 2011, Why Galaxies Care about AGB Stars II: Shining Examples and Common Inhabitants, 445, 3
Karakas A. I., Lattanzio J. C. 2014, PASA, 31, e030
Karakas A. I., Lattanzio J. C. 2014, PASA, 31, e030
Kobayashi C., Karakas A. I., Umeda H. 2011, MNRAS, 414, 3231
Matsuura M., et al., 2009, MNRAS, 396, 918
Matsuura M., Woods P. V., Owen P. J., 2013, MNRAS, 429, 2527
McSaveney J. A., Wood P. R., Scholz M., Lattanzio J. C., Hinkle K. H. 2007, MNRAS, 378, 1089
Meixner M. et al. 2006, AJ, 132, 2268
Meixner M. et al. 2010, A&A, 518, L71
Meixner M. et al. 2013, ApJ, 146, 62
Nanni A., Bressan A., Marigo P., Girardi L., 2013a, MNRAS, 434, 488
Nanni A., Bressan A., Marigo P., Girardi L., 2013b, MNRAS, 434, 2390
Nanni A. Bressan A. Marigo P. Girardi L., 2014, MNRAS, 438, 2328
Nenkova M., Ivezic Z., Elitzur M., 1999, in LPIContributions 969, Workshop on Thermal Emission Spectroscopy and Analysis of Dust, Disks, and Regoliths, ed. A. Sprague, D. K. Lynch, & M. Sitko (Houston, TX: Lunar and Planetary Institute), 20
Paczyński, B. 1970, Acta Astr., 20, 47
Piatti A.E., Geisler G., 2013, AJ, 145, 17
Renzini A., Voli M., 1981, A&A, 94, 175
Riebel D., Meixner M., Fraser O., Srinivasan S., Cook K., Vijh U., 2010, ApJ, 723, 1195
Riebel D., Srinivasan S., Sargent B., Meixner M., 2012, AJ, 753, 71
Romano D., Karakas A. I., Tosi M., Matteucci F. 2010, A&A 522, AA32
Schwarzschild M., Harm R. 1965, ApJ, 142, 855
Schwarzschild M., Harm R. 1967, ApJ, 145, 496
Skrutskie M. F. et al., 2006, AJ, 131, 1163
Schlegel D. J., Finkbeiner D. P., Davis M., 1998, ApJ, 500, 525
Schneider R., Valiante R., Ventura P., Dell'Agli F., Di Criscienzo M., Hirashita H., Kemper F. 2014, MNRAS, 442, 1440
Skrutskie M. 1998, in The Impact of Near-Infrared Sky Surveys on Galactic and Extragalactic Astronomy, Proc. of the 3rd Euroconference on Near-Infrared Surveys, ed. N. Epchtein, Astrophysics and Space Science library, 230, 11 (Dordrecht: Kluwer)
Srinivasan S. et al., 2009, AJ, 137, 4810
Valiante R., Schneider R., Bianchi S., Andersen A., Anja C., 2009, MNRAS, 397, 1661
Vassiliadis E., Wood P. R. 1993, ApJ, 413, 641
Ventura P., D'Antona F., Mazzitelli I., Gratton R. 2001, ApJ, 550, L65
Ventura P., D'Antona F., 2005, A&A, 431, 279
Ventura P., D'Antona F., 2008, A&A, 479, 805
Ventura P., D'Antona F., 2009, MNRAS, 499, 835
Ventura P., Di Criscienzo M., Schneider R., Carini R., Valiante R., D'Antona F., Gallerani S., Maiolino R., Tornambé A., 2012a, MNRAS, 420, 1442
Ventura P., Di Criscienzo M., Schneider R., Carini R., Valiante R., D'Antona F., Gallerani S., Maiolino R., Tornambé A., 2012b, MNRAS, 424, 2345
Ventura P., Dell'Agli F., Di Criscienzo M., Schneider R., Rossi C., La Franca F., Gallerani S., Valiante R., 2014a, MNRAS, 439, 977
Ventura P., Di Criscienzo, M., Carini R., D'Antona F., 2013, MNRAS, 431, 3642
Ventura P., Zeppieri A., Mazzitelli I., D'Antona F., 1998, A&A, 334, 953
Weisz D. R., Dolphin A. E., Skillman E. D., Holtzman J., Dalcanton J. J., Cole A. A., Neary K., 2013, MNRAS, 431, 364
Wood P. R., 2004, ApJ, 227, 220
Woods, P. M., Oliveira, J. M., Kemper, F., et al. 2011, MNRAS, 411, 1597
Zaritsky D., Harris J., Thompson I. B., Grebel E. K. 2004, AJ, 128, 1606
Zhukovska S., Gail H.-P., Trieloff M., 2008, A&A, 479, 453
Zhukovska S., Henning T., 2013, A&A, 555, 99